

OPEN

Preoperative Evaluation of Renal Cell Carcinoma by Using ^{18}F -FDG PET/CT

Miwako Takahashi, MD,* Haruki Kume, MD,† Keitaro Koyama, MD,* Tohru Nakagawa, MD,† Tetsuya Fujimura, MD,† Teppei Morikawa, MD,‡ Masashi Fukayama, MD,‡ Yukio Homma, MD,† Kuni Ohtomo, MD,* and Toshimitsu Momose, MD*

Purpose: This study aimed to characterize the FDG uptake of renal cell carcinoma (RCC) by the pathological subtype and nuclear grade.

Patients and Methods: We retrospectively identified patients who underwent ^{18}F -FDG PET and subsequent partial or radical nephrectomy for renal tumors. The relationships of the SUV of renal tumor with subtypes, nuclear grade, and clinicopathological variables were investigated.

Results: Ninety-two tumors were analyzed, including 52 low-grade (G1 and G2) and 18 high-grade (G3 and G4) clear cell RCC; 7 chromophobe, 5 papillary, and 1 unclassified RCC; and 9 benign tumors (7 angiomyolipoma and 2 oncocytoma). The SUVs of high-grade clear cell RCC (mean \pm SD, 6.8 ± 5.1) and papillary RCC (6.6 ± 3.7) were significantly higher than that of the controls (2.2 ± 0.3). The SUV of high-grade clear cell RCC was higher than that of low-grade tumors (median, 4.0 vs. 2.2; $P < 0.001$). The optimal SUV cutoff value of 3.0 helped to differentiate high-grade from low-grade clear cell RCC, with 89% sensitivity and 87% specificity. On multiple regression analysis, a high grade was the most significant predictor of SUV for clear cell RCC.

Conclusions: FDG uptake higher than that observed in normal kidney tissues suggests a high-grade clear cell RCC or papillary RCC subtype. FDG-PET using SUV may have a role in prediction of pathological grade of renal tumor.

Key Words: ^{18}F -FDG PET/CT, renal cell carcinoma, pathological nuclear grade

(*Clin Nucl Med* 2015;40: 936–940)

The number of patients diagnosed with renal tumor has been increasing with the extensive application of ultrasonography and computed tomography (CT).¹ Surgical resection remains necessary for a definitive diagnosis of renal tumor, but it is not always clinically beneficial, especially for elderly patients or those with severe comorbidities. For these patients, avoiding surgery and proceeding to active surveillance has become the mainstay of patient management.^{2,3} Without surgical intervention, the evaluation of tumor malignancy is helpful for treatment strategy decisions such as the timing of surgery or maintaining active surveillance.

F-18 fluorodeoxyglucose (FDG) positron emission tomography (PET) is a widely used effective modality for evaluating tumor

activity by estimating glucose metabolism. The usefulness of FDG-PET imaging in oncology is based on a correlation between glucose metabolism and the degree of tumor malignancy, which has been reported for various tumors.^{4–12}

Although we have observed differential FDG uptake in renal tumor, there are few studies concerning FDG-PET for renal cell carcinoma (RCC), most likely because of difficulties in differentiating the radioactivity of FDG accumulated in renal tumors from the radioactivity of FDG excreted via the urinary system during physiological processes. In addition, false-negative cases can lead to a low sensitivity for RCC detection.^{13–15} The use of FDG-PET for routine evaluation of renal tumors has not been recommended. However, recently dedicated PET-CT have improved image resolution and signal-to-noise ratio. In addition, attached-CT for photon attenuation correction provides anatomical information on FDG-PET images. A comparison of diagnostic CT and attached-CT facilitates the identification of renal tumors on FDG-PET images, which enable us to place region of interest (ROI) on renal tumor more accurately. Calculation semiquantitative values using these ROI help elucidate the characteristics of FDG uptake of a renal tumor.

In this study, we hypothesized that glycolytic metabolism would reflect tumor aggressiveness in renal tumors. Pathological findings such as histological subtype, nuclear grade, and TNM stage are the most widely used indicators for renal tumor aggressiveness.^{16–18} We investigated the correlation of preoperative renal tumor metabolic activity with tumor pathology. This study applied a semiquantitative value of metabolism as defined by the standardized uptake value (SUV) in a greater number of cases than previously investigated.

PATIENTS AND METHODS

This retrospective study was approved by the institutional review board. Consecutive patients who underwent FDG-PET at our hospital between April 2007 and August 2014 were included according to the following criteria: 1) renal tumor suspected on diagnostic CT, 2) partial nephrectomy or radical nephrectomy performed at our hospital within 6 months after FDG-PET, and 3) a blood glucose level of less than 150 mg/dL in patients undergoing FDG-PET.

FDG-PET studies were performed using a PET/CT scanner (Aquiduo; Toshiba Medical System, Otawara, Japan). Patients fasted for at least 5 hours before undergoing FDG-PET. Each patient was administered 296 MBq (8 mCi) ^{18}F -FDG intravenously until January 2011 and 4.5 MBq/kg (0.12 mCi/kg) thereafter. The scanner contains 24,336 lutetium oxyorthosilicate crystals in 39 detector rings and had an axial field of view of 16.2 cm and 82 transverse slices with a 2.0-mm thickness. The intrinsic full width at tenth-maximum (FWHM) spatial resolution in the center of the field of view was 4.3 mm, and the FWHM axial resolution was 4.7 mm. The sinogram was acquired using the 3-dimensional mode. The CT scan for photon attenuation correction was acquired with a tube current of 25 mA and a tube voltage of 120 kV, and a 2.5-min

Received for publication April 11, 2015; revision accepted April 26, 2015.

From the *Division of Nuclear Medicine, Department of Radiology, Graduate School of Medicine, The University of Tokyo, Tokyo, Japan, †Department of Urology, Graduate School of Medicine, The University of Tokyo, Tokyo, Japan, and ‡Department of Pathology, Graduate School of Medicine, The University of Tokyo, Tokyo, Japan.

Conflicts of interest and sources of funding: none declared.

Correspondence to: Toshimitsu Momose, MD, Division of Nuclear Medicine, Department of Radiology, University of Tokyo, 3-1 Hongo 7-Chome, Bunkyo-ku, Tokyo 113-8655, Japan. E-mail: tmomo-ky@umin.ac.jp.

Copyright © 2015 Wolters Kluwer Health, Inc. All rights reserved. This is an open-access article distributed under the term of the Creative Commons Attribution-Non Commercial-No Derivatives License 4.0 (CCBY-NC-ND), where it is permissible to download and share the work provided it is properly cited. The work cannot be changed in any way or used commercially.

ISSN: 0363-9762/15/4012-0936

DOI: 10.1097/RLU.0000000000000875

TABLE 1. Patient Characteristics According to Subtype and Grade

Histology and Grade	No. Patients (n)	Age (year)	Male: Female (n)
RCC			
Low-grade clear cell*	50	63 ± 13	42:10
High-grade clear cell†	18	64 ± 7	16:2
Chromophobe	7	55 ± 14	2:5
Papillary	5	73 ± 9	5:0
Unclassified	1	70	0:1
Benign tumor			
Angiomyolipoma	7	46 ± 10	4:3
Oncocytoma	2	70 ± 4	1:1

Values are means ± standard deviation.

*Low-grade clear cell, the tumor consists of nuclear grade G1 and G2 components.

†High-grade clear cell, the tumor contains of nuclear grade G3 or G4.

RCC indicates renal cell carcinoma.

emission scan per position was used. PET images were reconstructed using Fourier rebinning ordered subset expectation maximization iterative reconstruction, with 2 iterations and 8 subsets, and a 4-mm FWHM Gaussian filter was applied. The data were collected in a 128 × 128 × 41 matrix with a voxel size of 2.0 × 2.0 × 4.0 mm.

Renal tumors were identified on FDG-PET images by comparing FDG-PET images, and attached-CT and diagnostic CT images side by side. The diagnostic CT images were obtained separately as a routine evaluation. If needed, fused images of FDG-PET and attached-CT images were used. Metabolic tumor activity was calculated by placing a 10-mm diameter ROI on the area with the most intense activity within the tumor. The mean SUV of the ROI was applied for analysis. Similarly, the SUV of normal kidney tissue was calculated by placing the ROIs on the area with the maximum axial section of normal renal cortex and the minimum physiological activity of the renal calices. If the SUVs of normal kidney tissues showed no differences between subtypes, they were used as control data. All SUV measurements were normalized for patient body weight and for the time between injection and the data acquisition. Preoperative tumor size was measured as the maximum diameter on diagnostic CT axial images.

Pathological findings, including histological subtype, pT stage, and nuclear grading, were obtained. Nuclear grading was determined based on Fuhrman grading system.¹⁹ Clear cell RCCs were classified into 2 categories; tumors containing a nuclear G3 or G4 component and those consisting of G1 and G2 components (high- and low-grade clear cell RCC, respectively).

Statistical analyses were performed using SPSS 20.0 (IBM, Armonk, NY). To assess the significant differences between 2 groups, Student *t* test for parametric distribution or Mann–Whitney *U* test for nonparametric distribution were used. A chi-square test was used for the categorical data, and if the sample size was less than 5, the Fisher exact test was used. The Kruskal–Wallis test was used for multiple comparisons with adjusted *P* values. Receiver operating curve (ROC) analysis was used to determine the optimal cutoff values to calculate sensitivity and specificity. To determine the factors associated with the SUV value, univariate analysis of variables, including patient age, sex, blood glucose level at FDG injection, FDG dose, tumor size (i.e., maximum diameter), presence or absence of pathological invasion to neighboring tissues (pT3/4 or not), and nuclear grade, was performed. Any variables with a *P* < 0.1 on univariate analysis were subjected to multivariate regression analysis. For all test, 2-sided *P* < 0.05 was considered statistically significant.

RESULTS

Ninety-eight tumors from 93 patients including 5 patients (Patient 6, 9, 17, 48, and 55) with 2 lesions were identified. Among them, 6 tumors were difficult to delineate on PET images and were excluded from the analyses. The patient characteristics are shown in Table 1. The scatter plot of SUVs for each RCC subtype and grade is shown in Figure 1. The mean SUV of normal kidney tissues from all patients was calculated as 2.2 ± 0.3, and it was not significantly different across subtypes or grades (Kruskal–Wallis test; adjusted *P* = 0.628); therefore, this value was used as the control SUV.

The tumor size, SUVs, and comparisons with the control SUV are shown in Table 2. High-grade clear cell RCC and papillary RCC showed significantly higher SUVs compared with the control SUV (*P* < 0.001 and *P* = 0.007, respectively; Kruskal–Wallis test). Differentiation of RCC from benign tumors at the SUV cutoff value of 2.2 provided a sensitivity of 65%, specificity of 89%, and an area under the curve (AUC) of 0.70.

In clear cell RCC, high-grade clear cell RCC had a significantly greater tumor size and a higher SUV value compared with low-grade clear cell RCC (*P* = 0.003 and *P* < 0.001, respectively). An SUV cutoff value of 3.0 helped to differentiate high-grade from low-grade clear cell RCC, with a sensitivity of 89%, specificity of 87%, and an AUC of 0.96. Using a cutoff value of 40 mm as the maximum tumor diameter, the sensitivity, specificity, and AUC were 78%, 54%, and 0.75, respectively.

For regression analysis on clear cell RCC, we excluded 2 extreme outliers (SUVs, 21.7 and 13.8 [patients 1 and 89, respectively]). Extreme outliers were defined as a value 2-fold higher than that of the interquartile range. On the univariate analysis,

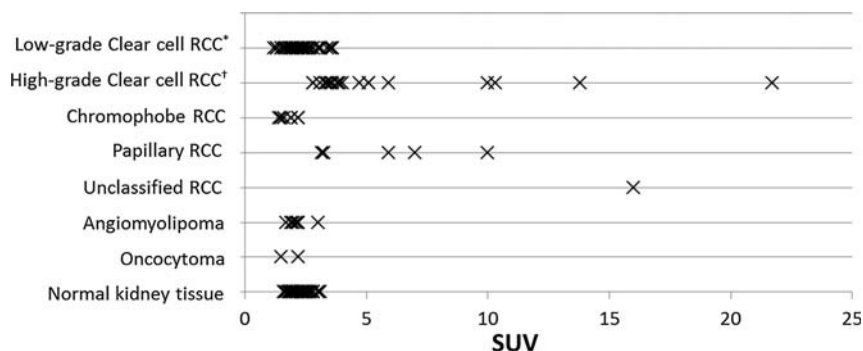


FIGURE 1. Scatter plot of the standardized uptake values (SUVs) according to the pathological subtype and grade and those of normal kidney tissue. *Low-grade clear cell, the tumor consists of nuclear grade G1 and G2 components; †High-grade, the tumor contains of nuclear grade G3 or G4 components.

TABLE 2. Tumor Characteristics and Comparisons of SUVs Between Tumors and Control

Histology and Grade	No. Tumors (n)	Tumor Size (mm)	SUV		SUV Comparison with Control
		Mean ± SD	Mean ± SD	Median (range)	Adjusted <i>P</i> *
RCC					
Low-grade clear cell	52	40 ± 19	2.3 ± 0.6	2.2 (1.2–3.6)	1.000
High-grade clear cell	18	61 ± 25	6.2 ± 4.9	4.0 (2.8–21.7)	<0.001
Chromophobe	7	38 ± 32	1.8 ± 0.3	1.9 (1.4–2.2)	1.000
Papillary	5	53 ± 41	5.9 ± 2.9	5.9 (3.2–10.0)	0.007
Unclassified	1	162	16.0	16.0	N.D.
Benign Tumor					
Angiomyolipoma	7	20 ± 9	2.2 ± 0.4	2.1 (1.7–3.0)	1.000
Oncocytoma	2	24 ± 1	1.9 ± 0.5	1.9 (1.5–2.2)	ND

*Kruskal-Wallis test.

SUV indicates standardized uptake value; SD, standard deviation; RCC, renal cell carcinoma; ND, not done.

independent variables with $P < 0.1$ were high-grade RCC on nuclear grading, high T stage (pT3 and 4), and the tumor size, with the SUV of clear cell RCC being the dependent variable. The results of the multiple regression analysis are shown in Table 3. A high-grade finding had the highest influence on SUV with a β -value of 0.41.

Representative cases of low- and high-grade clear cell RCC are shown in Figure 2.

DISCUSSION

FDG accumulation increases with the degree of malignancy in various tumors,^{4–12} but it has scarcely been reported for RCC. This study investigated FDG uptake of renal tumors using semi-quantitative SUV values in a larger patient population than that used in previous studies.^{13–15} In clear cell RCC, we found that high-grade clear cell RCC showed higher metabolism than low-grade clear cell RCC, and high-grade on pathological nuclear grading was the most significant predictive value of SUV. According to the histological subtypes and the grade, high-grade clear cell RCC and papillary RCC showed higher SUV than normal kidney tissues; in contrast, low-grade clear cell RCC and chromophobe RCC did not show differences in the SUV when compared with normal kidney tissues.

Our result with 70 cases of clear cell RCC is consistent with previous reports using an SUV evaluation method and supports them with visual evaluation. Ho et al. investigated 36 cases of clear cell RCC and showed a significantly higher ratio of the maximum

SUV (SUV of the lesion to that of the normal kidney) in high-grade RCC compared with low-grade RCC¹⁵; these findings are similar to those obtained in this study. In a previous visual evaluation of 15 RCC tumors, visible tumors showed a higher nuclear grade compared with nonvisible tumors.¹⁴ Aide et al. also showed that the visible FDG-positive renal tumors tended to be pathological high-grade tumors.¹³ Nuclear grade is a well-established prognostic factor that showed a significant association with disease-specific survival for clear cell RCC.^{18,20} In addition, higher FDG accumulation of RCC relates with a less favorable prognosis.^{15,21} In light of these findings, it was suggested that the metabolic activity was associated with aggressiveness of clear cell RCC, as hypothesized here.

The total sensitivity of differentiating RCC from benign lesions with the cutoff value of SUV 2.2 was 68% in this study. Previous studies showed that FDG-PET sensitivity for RCCs ranged widely from 32% to 90%^{13–15,22–27}; some studies suggested that the low sensitivity was attributed to false-negative findings, indicating that the FDG uptake of RCCs were equivalent to or lower than that of the normal kidney parenchyma.^{14,15,24,27} Ho et al. reported that all 7 chromophobe RCC cases in their study were negative for FDG uptake.¹⁵ In our study, the SUVs of chromophobe RCC and low-grade clear cell RCC largely overlapped with those of normal kidney tissues. The previously reported insufficient sensitivity for RCC by using FDG-PET could be due to the relatively low FDG uptake by chromophobe RCC and low-grade clear cell RCC.

Active surveillance of RCC is an important option in patients with high surgical risk; therefore, preoperative noninvasive imaging is expected to provide a more accurate estimation of tumor

TABLE 3. Multiple Regression Analysis for SUV of Clear Cell RCC

Independent variable	Dependent variable: SUV of clear cell RCC			
	Beta	SE	β	<i>P</i>
$(R^2 = 0.49)$				
Intercept	1.97	0.32		<0.001
High-grade (G3 and G4), (vs. G1 and G2)	1.51	0.47	0.41	0.002
High T stage (T3 and T4)	1.11	0.50	0.29	0.031
Tumor size (continuous, mm)	0.01	0.01	0.10	0.356

R^2 = R-square (the coefficient of multiple determination) of the model; Beta = unstandardized regression coefficient; SE = standard error for each independent variable; β = standardized regression coefficient.

SUV indicates standardized uptake value; RCC, renal cell carcinoma.

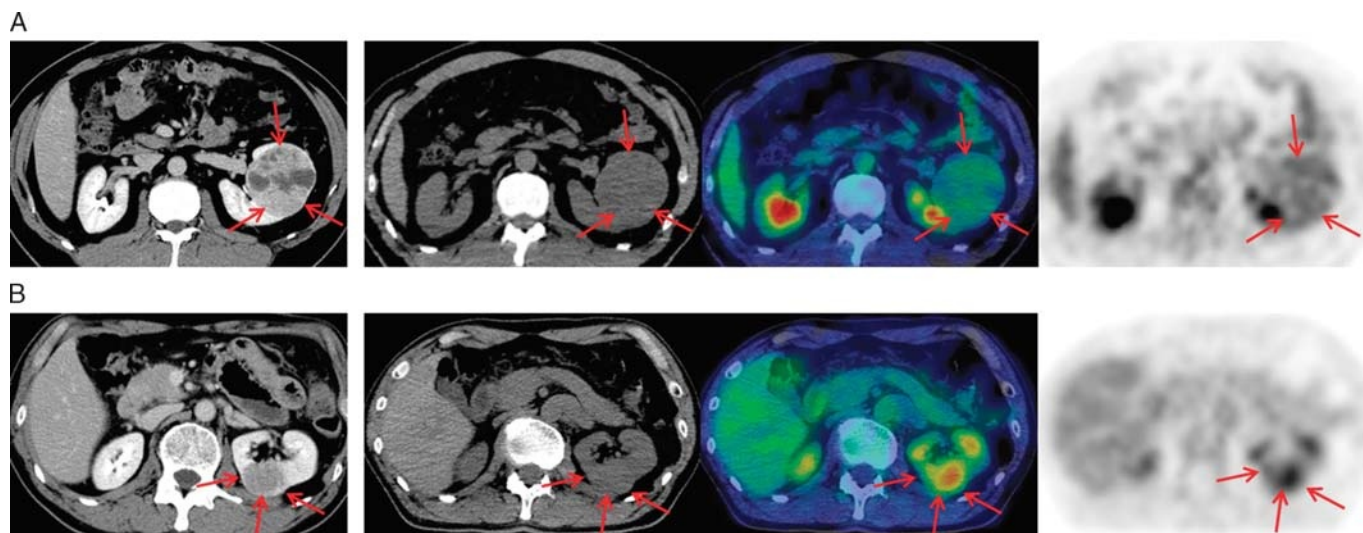


FIGURE 2. Representative cases. The images from left-to-right are as follows: diagnostic contrast-enhanced computed tomography (CT) image, attached-CT images for photon attenuation correction, fusion of PET and attached-CT images, and a PET image. **A**, Images of a tumor in a 44-year-old man with a low-grade clear cell RCC in the left kidney. The tumor size on CT is 69 × 64 mm, and the standardized uptake value (SUV) is 2.3. **B**, Images of a tumor in a 70-year-old man with a high-grade clear cell RCC in the left kidney. The tumor size on CT is 38 × 35 mm, and the SUV is 5.1.

aggressiveness. Our findings suggest that renal tumors with high FDG accumulation are likely to be high-grade clear cell RCC or papillary RCC. In the clinical setting, CT is the primary imaging modality used for preoperative evaluation, and images frequently show a characteristic enhanced pattern for clear cell RCC.^{28,29} When clear cell RCC is suspected on contrast-enhanced CT, high FDG accumulation would suggest a high-grade tumor more accurately than tumor size on CT alone.

FDG accumulation relies on the first steps of glucose metabolism pathway, which includes components such as glucose transporters (GLUTs), hexokinase (HK), and glucose-6 phosphatase (G6Pase). Among them, GLUT-1 was the most significant factor for FDG uptake in various tumors. Overexpression of GLUT-1 has been demonstrated in clear cell RCC,^{30,31} but a positive correlation between the level of GLUT-1 expression and the nuclear grade has not been found.^{23,30} However, on immunohistochemical studies, subtypes such as GLUT-5 have shown stronger staining in clear cell RCC than that observed in other subtypes.³² Furthermore, considering the role of gluconeogenesis in the kidneys, which is comparative to that of the liver,³³ G6Pase may be related with the tumor glucose metabolism. For hepatocellular carcinoma (HCC), SUV was higher for high-grade HCC compared with low-grade HCC, and the ratio of G6Pase to HK was lower in high-grade HCC compared with low-grade HCC.¹² For FDG kinetics in most tumors, G6Pase is considered negligible, but in renal tumors, G6Pase activity and other types of GLUTs may significantly relate to FDG accumulation.

This study included 5 cases of papillary RCC, 4 of which were type 2 and one was undetermined. A few cases of papillary RCC have been included in previous studies with FDG-PET. Ho et al. reported on a case of FDG-negative papillary RCC that was pathologically identified as type 1.¹⁵ Although their subtype was not described, 3 cases of papillary RCCs with FDG-negative characteristics were found in other previous studies.^{26,27} Therefore, the high FDG uptake of papillary RCC observed in the present study could be associated with type 2 papillary RCCs. Genetic alteration of type 2 papillary RCC has been investigated through the hereditary renal cancer syndrome. Germline mutations have been

identified in the gene that encodes one of the tricarboxylic acid cycle enzymes, fumarate hydratase (FH).³⁴ Insufficient FH leads to stabilization of hypoxia-inducible factor, resulting in overexpression of GLUT.³⁵ A case study of a patient with sporadic onset of *FH*-deficient type 2 papillary RCC showed increased FDG uptake in peritoneal carcinomatosis on FDG-PET, which was performed at recurrence after surgical resection of RCC and surrounding involved organs. In an immunohistochemical study of 26 cases of papillary RCC, 10 showed high GLUT-1 expression, and patients tended to show a poor prognosis compared with those with low GLUT-1 expression, although the trend was not significant.³⁰ Patients with type 2 papillary RCC have a poor prognosis compared with those with type 1 papillary RCC.³⁶ From this, it can be inferred that the high degree of metabolic activity of papillary RCC was attributed to the overexpression of GLUT and potentially represents the malignant aggressiveness of type 2 papillary RCC. Our sample size is small, and the clinicopathological implications of the degree of metabolism in papillary RCC require further study in a large cohort.

In the present study, 6 tumors were excluded from the analysis because they could not be clearly identified on PET images, mostly because the degrees of FDG accumulation in small tumors was almost equivalent to that in the surrounding normal parenchyma, and these tumors did not show exophytic growth. All these tumors were low-grade clear cell RCC ranging from 12 to 20 mm in size. In addition, 1 tumor was affected by spill-in phenomenon from neighboring high radioactive retention in the calyx of the kidneys. The spill-in phenomenon was attributed to the partial volume effect (PVE), a specific problem for PET imaging. PVE also causes underestimation of measured radioactivity on PET images. All lesions included in the present study had a minimum diameter of 10 mm, but underestimation of radioactivity can occur depending on the size of up to approximately 4 cm in diameter.³⁷

To overcome the disadvantages of FDG, specific tracers for RCC or tracers that are not excreted via the urinary system would be ideal. I-124 girentuximab is a radiolabeled antibody that binds to a specific antigen expressed on the cell surface of clear cell RCC cells, and it is reported to have a favorable diagnostic

performance for clear cell RCC.³⁸ C-11 acetate, which is not excreted via the urinary system, was reported as having improved sensitivity for RCC when compared with ¹⁸F-FDG.^{15,27,39} However, ¹¹C-acetate showed intensive accumulation in angiomyolipoma and no significant difference between high- and low-grade clear cell RCC.¹⁵ Therefore, using these tracers before surgical procedures may compliment FDG to provide information that is more accurate for patients with renal tumors.

A limitation of this study is the small sample size for the histological subtypes of nonclear cell RCC; therefore, we were not able to investigate the relationship of the SUV with nonclear cell RCC by pathological grade.

CONCLUSIONS

FDG uptake of a renal tumor higher than that of normal kidney tissues suggests the presence of high-grade clear cell RCC or papillary RCC. When clear cell RCC is suspected, high FDG uptake indicates a pathologically high nuclear grade. Our results suggest that high FDG uptake is associated with the pathological grade of a renal tumor, although the characterization of non-clear cell RCCs requires further study in a larger patient population.

ACKNOWLEDGMENTS

The authors thank Seiji Kato, Yoshiharu Sekine, Michiharu Sekimoto, and Katsuji Nishida for the professional support with the nuclear medicine technology.

REFERENCES

- Chow WH, Dong LM, Devesa SS. Epidemiology and risk factors for kidney cancer. *Nat Rev Urol*. 2010;7:245–257.
- Rosales JC, Haramis G, Moreno J, et al. Active surveillance for renal cortical neoplasms. *J Urol*. 2010;183:1698–1702.
- Gontero P, Joniau S, Oderda M, et al. Active surveillance for small renal tumors: have clinical concerns been addressed so far? *Int J Urol*. 2013;20:356–361.
- Endo M, Nakagawa K, Ohde Y, et al. Utility of ¹⁸FDG-PET for differentiating the grade of malignancy in thymic epithelial tumors. *Lung Cancer*. 2008;61:350–355.
- Heudel P, Cimarelli S, Montella A, et al. Value of PET-FDG in primary breast cancer based on histopathological and immunohistochemical prognostic factors. *Int J Clin Oncol*. 2010;15:588–593.
- Kadota K, Colovos C, Suzuki K, et al. FDG-PET SUVmax combined with IASLC/ATS/ERS histologic classification improves the prognostic stratification of patients with stage I lung adenocarcinoma. *Ann Surg Oncol*. 2012;19:3598–3605.
- Watanabe Y, Suefuji H, Hirose Y, et al. ¹⁸F-FDG uptake in primary gastric malignant lymphoma correlates with glucose transporter 1 expression and histologic malignant potential. *Int J Hematol*. 2013;97:43–49.
- Rakheja R, Makis W, Skamene S, et al. Correlating metabolic activity on ¹⁸F-FDG PET/CT with histopathologic characteristics of osseous and soft-tissue sarcomas: a retrospective review of 136 patients. *AJR Am J Roentgenol*. 2012;198:1409–1416.
- Kaschten B, Stevenaert A, Sadzot B, et al. Preoperative evaluation of 54 gliomas by PET with fluorine-18-fluorodeoxyglucose and/or carbon-11-methionine. *J Nucl Med*. 1998;39:778–785.
- Borgwardt L, Hojgaard L, Carstensen H, et al. Increased fluorine-18-2-fluoro-2-deoxy-D-glucose (FDG) uptake in childhood CNS tumors is correlated with malignancy grade: a study with FDG positron emission tomography/magnetic resonance imaging coregistration and image fusion. *J Clin Oncol*. 2005;23:3030–3037.
- Kubota K, Okasaki M, Minamimoto R, et al. Lesion-based analysis of (18)F-FDG uptake and (111)In-Pentetreotide uptake by neuroendocrine tumors. *Ann Nucl Med*. 2014;28:1004–1010.
- Torizuka T, Tamaki N, Inokuma T, et al. In vivo assessment of glucose metabolism in hepatocellular carcinoma with FDG-PET. *J Nucl Med*. 1995;36:1811–1817.
- Aide N, Cappele O, Bottet P, et al. Efficiency of [(18)F]FDG PET in characterising renal cancer and detecting distant metastases: a comparison with CT. *Eur J Nucl Med Mol Imaging*. 2003;30:1236–1245.
- Ozulkar T, Ozulkar F, Ozbek E, et al. A prospective diagnostic accuracy study of F-18 fluorodeoxyglucose-positron emission tomography/computed tomography in the evaluation of indeterminate renal masses. *Nucl Med Commun*. 2011;32:265–272.
- Ho CL, Chen S, Ho KM, et al. Dual-tracer PET/CT in renal angiomyolipoma and subtypes of renal cell carcinoma. *Clin Nucl Med*. 2012;37:1075–1082.
- Gudbjartsson T, Hardarson S, Petursdottir V, et al. Histological subtyping and nuclear grading of renal cell carcinoma and their implications for survival: a retrospective nation-wide study of 629 patients. *Eur Urol*. 2005;48:593–600.
- Volpe A, Patard JJ. Prognostic factors in renal cell carcinoma. *World J Urol*. 2010;28:319–327.
- Ficarra V, Martignoni G, Maffei N, et al. Original and reviewed nuclear grading according to the Fuhrman system: a multivariate analysis of 388 patients with conventional renal cell carcinoma. *Cancer*. 2005;103:68–75.
- Fuhrman SA, Lasky LC, Limas C. Prognostic significance of morphologic parameters in renal cell carcinoma. *Am J Surg Pathol*. 1982;6:655–663.
- Rioux-Leclercq N, Karakiewicz PI, Trinh QD, et al. Prognostic ability of simplified nuclear grading of renal cell carcinoma. *Cancer*. 2007;109:868–874.
- Ferda J, Ferdova E, Hora M, et al. ¹⁸F-FDG-PET/CT in potentially advanced renal cell carcinoma: a role in treatment decisions and prognosis estimation. *Anticancer Res*. 2013;33:2665–2672.
- Ramdave S, Thomas GW, Berlangieri SU, et al. Clinical role of F-18 fluorodeoxyglucose positron emission tomography for detection and management of renal cell carcinoma. *J Urol*. 2001;166:825–830.
- Miyakita H, Tokunaga M, Onda H, et al. Significance of ¹⁸F-fluorodeoxyglucose positron emission tomography (FDG-PET) for detection of renal cell carcinoma and immunohistochemical glucose transporter 1 (GLUT-1) expression in the cancer. *Int J Urol*. 2002;9:15–18.
- Kang DE, White RL Jr, Zuger JH, et al. Clinical use of fluorodeoxyglucose F 18 positron emission tomography for detection of renal cell carcinoma. *J Urol*. 2004;171:1806–1809.
- Kumar R, Chauhan A, Lakhani P, et al. 2-Deoxy-2-[¹⁸F]fluoro-D-glucose-positron emission tomography in characterization of solid renal masses. *Mol Imaging Biol*. 2005;7:431–439.
- Nakhoda Z, Torigian DA, Saboury B, et al. Assessment of the diagnostic performance of (18)F-FDG-PET/CT for detection and characterization of solid renal malignancies. *Hell J Nucl Med*. 2013;16:19–24.
- Oyama N, Ito H, Takahara N, et al. Diagnosis of complex renal cystic masses and solid renal lesions using PET imaging: comparison of ¹¹C-acetate and ¹⁸F-FDG PET imaging. *Clin Nucl Med*. 2014;39:e208–e214.
- Zokalj I, Marotti M, Kolaric B. Pretreatment differentiation of renal cell carcinoma subtypes by CT: the influence of different tumor enhancement measurement approaches. *Int Urol Nephrol*. 2014;46:1089–1100.
- Kim JK, Kim TK, Ahn HJ, et al. Differentiation of subtypes of renal cell carcinoma on helical CT scans. *AJR Am J Roentgenol*. 2002;178:1499–1506.
- Lidgren A, Bergh A, Grankvist K, et al. Glucose transporter-1 expression in renal cell carcinoma and its correlation with hypoxia inducible factor-1 alpha. *BJU Int*. 2008;101:480–484.
- Suganuma N, Segade F, Matsuzo K, et al. Differential expression of facilitative glucose transporters in normal and tumour kidney tissues. *BJU Int*. 2007;99:1143–1149.
- Aparicio LM, Villamil VM, Calvo MB, et al. Glucose transporter expression and the potential role of fructose in renal cell carcinoma: A correlation with pathological parameters. *Mol Med Rep*. 2010;3:575–580.
- Gerich JE, Meyer C, Woerle HJ, et al. Renal gluconeogenesis: its importance in human glucose homeostasis. *Diabetes Care*. 2001;24:382–391.
- Toro JR, Nickerson ML, Wei MH, et al. Mutations in the fumarate hydratase gene cause hereditary leiomyomatosis and renal cell cancer in families in North America. *Am J Hum Genet*. 2003;73:95–106.
- Isaacs JS, Jung YJ, Mole DR, et al. HIF overexpression correlates with biallelic loss of fumarate hydratase in renal cancer: novel role of fumarate in regulation of HIF stability. *Cancer Cell*. 2005;8:143–153.
- Waldert M, Haitel A, Marberger M, et al. Comparison of type I and II papillary renal cell carcinoma (RCC) and clear cell RCC. *BJU Int*. 2008;102:1381–1384.
- Soret M, Bacharach SL, Buvat I. Partial-volume effect in PET tumor imaging. *J Nucl Med*. 2007;48:932–945.
- Divgi CR, Uzzo RG, Gatsonis C, et al. Positron emission tomography/computed tomography identification of clear cell renal cell carcinoma: results from the REDECT trial. *J Clin Oncol*. 2013;31:187–194.
- Shreve P, Chiao PC, Humes HD, et al. Carbon-11-acetate PET imaging in renal disease. *J Nucl Med*. 1995;36:1595–1601.